Binding to DNA Purine Base and Structure−Activity Relationship of a Series of Structurally Related Ru(II) Antitumor Complexes: A Theoretical Study

Jin-Can Chen,[†,‡] Lan-Mei Chen,[†] Lian-Cai Xu,[†] Kang-Cheng Zheng,*[,†] and Liang-Nian Ji*[,†]

Key Laboratory of Bioinorganic and Synthetic Chemistry of the Ministry of Education, School of Chemistry and Chemical Engineering, Sun Yat-Sen University, Guangzhou, 510275, People's Republic of China, and Analytic Centre of Guangdong Medical College, Zhanjiang, 524023, People's Republic of China

Received: December 16, 2007; Revised Manuscript Received: April 7, 2008

The thermodynamics of the binding of a series of structurally related Ru(II) antitumor complexes, that is, α-[Ru(azpy)$_2$Cl$_2$] **1**, *β*-[Ru(azpy)$_2$Cl$_2$] **2**, α-[Ru(azpy)(bpy)Cl$_2$] **3**, and *cis*-[Ru(bpy)$_2$Cl$_2$] **4** to DNA purine bases (gunine, adenine at N7 site) has been studied by using the DFT method. The binding of imine form of 9-methyladenine (9-MeAde) to the Ru(II) moiety in a didentate fashion via its N6 and N7 atoms was also considered. The geometrical structures of the DNA model base adducts were obtained at the B3LYP/(LanL2DZ + 6−31G(d)) level in vacuo. The following exact single-point energy calculations were performed at the B3LYP/(LanL2DZ(f)+6−311+G(2d, 2p)) level both in vacuo and in aqueous solution using the COSMO model. The bond dissociation enthalpies and free energies, reaction enthalpies and free energies both in the gas phase and in aqueous solution for all considered Ru(II)-DNA model base adducts were obtained from the computations. The calculated bond dissociation enthalpies and free energies allow us to build a binding affinity order for the considered Ru(II)-DNA model base adducts. The theoretical results show that the guanine N7 is a preferred site for this series of complexes and support such an experimental fact that α-[Ru(azpy)(bpy)(9-EtGua)H$_2$O]$^{2+}$ (**3**-(9-EtGua)) is isomerized to α′-[Ru(azpy)(bpy)(9-EtGua)H$_2$O]$^{2+}$ (**3′**-(9-EtGua)). On the basis of structural and thermodynamical characteristics, the possible structure−activity relationship was obtained, and the distinct difference in cytotoxicities of this series of structurally related antitumor complexes was explained theoretically.

1. Introduction

After the successful development of cisplatin (*cis*-diamminedichloroplatinum(II), *cis*-[PtCl$_2$(NH$_3$)$_2$]) as a cancer drug,[1] several ruthenium complexes have aroused a great interest for their potential use as therapeutic anticancer agents with lower toxicity than the platinum counterparts[2–5] and have been under investigation more recently.

The cytotoxic activities of the [RuL$_2$Cl$_2$] (L = 2-phenylazopyridine, *o*-tolylazopyridine, and 4-methyl-2-phenylazopyridine) complexes against a series of human tumor cell lines have been reported;[6] the different isomeric complexes show distinct difference in cytotoxicities. In particular, the α isomer, α-[Ru(azpy)$_2$Cl$_2$] (azpy = 2-phenylazopyridine), has been reported to show a remarkably high cytotoxicity, even more pronounced than cisplatin in most of the tested cell lines, and the *β* isomer shows a cytotoxicity of a factor of 10 lower than the α isomer in the same panel of cell lines.[6,7] Most interestingly, the structurally related complex *cis*-[Ru(bpy)$_2$Cl$_2$] is inactive,[8] and the mixed-ligand compound α-[Ru(azpy)(bpy)Cl$_2$] shows a low or moderate cytotoxicity in several cell lines.[9] At present, although such series of anticancer-active ruthenium complexes have shown antitumor, cytotoxic, or antimetastatic activity, no clear structure−activity relationship (SAR) has been found yet.

These ruthenium complexes are generally octahedral and six-coordinated, and thus their binding to DNA base-pairs is sterically much more constrained than that of the square-planar four-coordinated platinum complexes, so such complexes may act in a different way from that of cisplatin, which is known to its binding to two neighboring guanine bases in DNA.[10] For cisplatin and carboplatin, aquation process is believed to be the key activation step before the drug reaches its intracellular target, [11,12] since the aqua complexes are generally much more reactive toward DNA bases than the parent chloro complex.[13–15] Some experiments show that such a case seems to exist also for the ruthenium complex,[16] such as [ImH][*trans*-RuCl$_4$(DMSO)(Im)] (NAMI-A; Im = imidazole, DMSO = dimethyl sulfoxide),[17–22] [IndH][*trans*-RuCl$_4$Ind$_2$] (KP1019, Ind = indazole)[23] and [ImH][*trans*-RuCl$_4$Im$_2$] (ICR, Im = imidazole).[23–26] These Ru(III) drugs lose their chloride ligands and transform into the more reactive aquated species which then undergo water substituted by one or two DNA nucleobases.

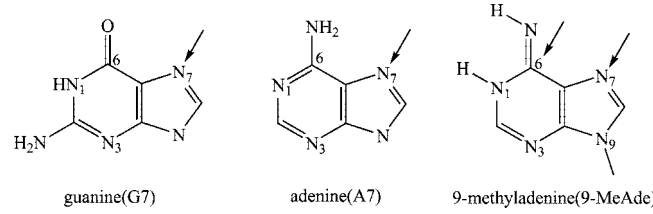

Figure 1. Schematic structures of DNA purine base guanine (G7), adenine (A7), and 9-methyladenine (9-MeAde).

It is generally accepted that DNA might be the target for anticancer-active ruthenium complexes.[27,28] Increasing evidence in the literatures show that the antitumor properties of many of these ruthenium complexes can be attributed to their interactions with DNA nucleobases.[29–32] Moreover, many experimental evidence indicate that the preferred binding target of ruthenium complexes is the N7 site of guanine (Figure 1), although binding

* Corresponding authors. E-mail: ceszkc@mail.sysu.edu.cn (K.-C.Z.) and cesjln@mail.sysu.edu.cn (L.-N.J.). Phone: 0086-20-84110696. Fax: 0086-20-84112245.
† Sun Yat-Sen University.
‡ Analytic Centre of Guangdong Medical College.

10.1021/jp711799g CCC: $40.75
Published on Web 07/17/2008

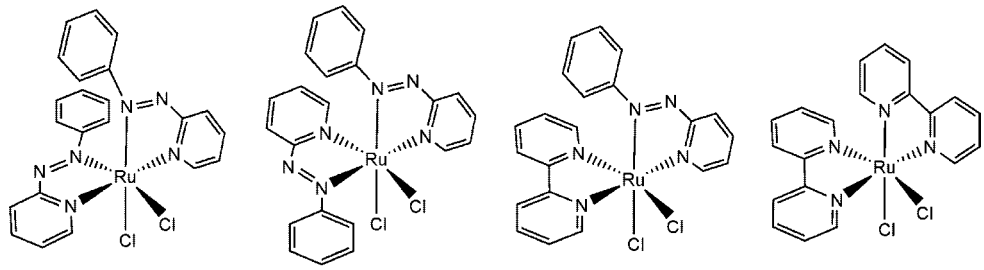

1 2 3 4

Figure 2. Schematic structures of α-[Ru(azpy)$_2$Cl$_2$] **1**, *β*-[Ru(azpy)$_2$Cl$_2$] **2**, α-[Ru(azpy)(bpy)Cl$_2$] **3**, and *cis*-[Ru(bpy)$_2$Cl$_2$] **4**.

to adenine and cytosine may also occur.[29–34] Therefore, a clear understanding of the interaction of ruthenium complexes with DNA model bases is very important to reveal the action mechanism of ruthenium-based drugs. More recently, several Ru(II) complexes coordinated to DNA-model bases/derivatives have been synthesized and studied by NMR and X-ray diffraction.[9,35–38] The experimental results showed that the hydrolyzed species of complexes α-[Ru(azpy)$_2$Cl$_2$], *cis*-[Ru(bpy)$_2$Cl$_2$], and α-[Ru(azpy)(bpy)Cl$_2$] can bind to only one 9-EtGua model base coordinating via the N7 atom.[9,37,38] But with respect to another DNA purine base (adenine), it has been found that it coordinates to the complexes α-[Ru(azpy)$_2$Cl$_2$] and *cis*-[Ru(bpy)$_2$Cl$_2$] in the rare imine form via N6, N7-didentate coordination.[35,36] Moreover, it was found that the guanine derivatives in Ru(II)-azpy complexes have more orientations than the related *cis*-[Ru(bpy)$_2$Cl$_2$] species,[35,36,38,39] and the bifunctional coordination of the purine model base 1-methylbenzimidazole to the α-isomer has sterically less hindrance than the coordination to the *β* isomer and *cis*-[Ru(bpy)$_2$Cl$_2$].[38–41] The differences in accessibilities of the two potential coordination sites for biologically relevant nitrogen bases may play a key role in causing the biological activities of antitumor-active ruthenium complexes.

In comparison with the experimental efforts, so far, the direct theoretical studies aimed at elucidating mode of action of ruthenium-based drugs (including the hydrolysis mechanism and binding to DNA-model bases) at the ab initio quantum mechanical (QM) level are still quite scarce. In a recent DFT study, the hydrolysis processes of the two Ru(III) antitumor complexes were reported by the current authors.[42,43] In our early work, the electronic and geometric structures as well as the structure−activity relationship (SAR) of the parent isomers, that is, α-, *β*-, *γ*-, *δ*-, and *ε*-[Ru(azpy)$_2$Cl$_2$] as well as their substitutive derivatives, that is, α-, *β*-, and *γ*-[Ru(mazpy)$_2$Cl$_2$] (mazpy = 4-methyl-2-phenylazopyridine), were also investigated systemically.[44,45] Recently, the thermodynamics of the binding of the antitumor ammine, amine, and immine complexes of ruthenium(II) and ruthenium(III) to DNA and peptides was studied computationally using model molecules, and a binding affinity order for the considered nucleic acid or protein binding sites was obtained.[46] In addition, the aquation processes (substitution of X by H_2O) of ruthenium(II) arene complexes of the type of [(η^6-arene)Ru(ethylenediamine)(X)]$^{n+}$ were explored using the DFT(PW91) method.[47] More recently, the study on structural and energetic properties of organometallic ruthenium(II) diamine anticancer compounds and their interaction with nucleobases using the DFT (BP86) and MP2 calculations together with Car−Parrinello molecular dynamics has been published.[48]

At present, with respect to this kind of Ru(II)-azpy anticancer complex presented above, though many experimental studies on the interaction between the complex and the biomolecular target (like DNA-model bases) have been well-reported, [9,35–38,40,41] to the best of our knowledge, so far, a comprehensive theoretical report on the reaction of such Ru(II) complexes with DNA model bases has not been found. A deeper insight into such interaction is of importance for understanding the drug's function and its action mechanism within the cell.

In this work, we select a series of structurally related complexes, that is, α-[Ru(azpy)$_2$Cl$_2$] **1**, *β*-[Ru(azpy)$_2$Cl$_2$] **2**, α-[Ru(azpy)(bpy)Cl$_2$] **3**, and *cis*-[Ru(bpy)$_2$Cl$_2$] **4** (Figure 2), to carry out a theoretical study applying the density functional theory (DFT) method.[49–52] This paper mainly focuses on revealing the differences on the structural characteristics as well as the thermodynamical properties of the Ru(II)-DNA model base adducts, in order to build a binding affinity order for the considered Ru(II)-DNA adducts both in the gas phase and in aqueous solution. Hereby, the structure−activity relationship (SAR) is discussed in detail, and thus a new insight into understanding theoretically the distinct difference in cytotoxicities of this series of structurally related Ru(II) antitumor complexes is offered.

2. Computational Details

All geometry optimizations for the ground states of all of the studied Ru(II)-DNA model base adducts, Ru(II) fragments, and the considered DNA purine bases were carried out using density functional theory (DFT)-B3LYP approach, that is, the Becke three-parameter hybrid exchange functional (B3)[53] and the Lee, Yang, and Parr (LYP) correlation functional.[54] The singlet state of these Ru(II) complexes was employed. [55] The LanL2DZ + 6−31G(d) hybrid basis set, that is, the effective core potential basis set LanL2DZ [56–58] for Ru and the standard split valence basis set 6−31G(d) [59,60] for C, N, O, H, and Cl atoms was used throughout this work for the geometry optimizations in vacuo. The frequency calculation was also carried out to verify the stable configuration of each species and to obtain the zero-point energy (ZPE) and the thermal energy contributions at 298.15 K and 1 atm.

To obtain accurate energies for the thermodynamics properties, single-point energies were further calculated in vacuo and in aqueous solution adopting the conductor-like screening model COSMO [61,62] using a higher basis set of LanL2DZ(f)+6−311+G(2d, 2p); that is, the LanL2DZ basis set including *f* polarization function ($\zeta_f = 1.235$)[63] was used for Ru (hereafter called LanL2DZ(f)), and 6−311+G(2d, 2p) basis set was used for the other atoms. ZPE corrections, thermal corrections to the enthalpy and Gibbs free energy terms and solvation free energies (ΔG_{solv}) have been employed to exactly calculate Gibbs free energies for the Ru−B bond formation at 298 K both in the gas phase (ΔG^{298}(gas)), and in solution (ΔG^{298}(aq)). We also evaluated the gas-phase bond formation enthalpies, ΔH^{298}(gas), and an approximate estimate of the bond formation enthalpies

in aqueous solution following the equation of $\Delta H^{298}(aq) = \Delta H^{298}(gas) + \Delta\Delta G_{solv}$. In addition, we found that different calculation methods and solvation models can affect the solvation free energies significantly, and thus affect the results of thermodynamic properties. Since no experimental value is available for all of the species in our calculations, we test our calculations for the solvation free energies of adenine and guanine using two solvation models, CPCM[64–66] and COSMO, and a comparison between our calculational results and other authors'[46,67–74] was given in Supporting Information (Table S1). The data in Table S1 clearly show that our calculational solvation free energies of adenine and guanine at the level of B3LYP/6−311+G(2d,2p)//B3LYP/6−31G(d) using COSMO model are in a good agreement with the recent report using the DFT calculations.[46,73] So the single-point energy of each species in aqueous solution was calculated using COSMO model.

In order to support that guanine is superior to adenine for coordination to Ru(II) hydrolyzed species kinetically, we take the reaction of α-$[Ru(azpy)_2(H_2O)_2]^{2+}$ (**1**-$(H_2O)_2$) with G7 (A7) as an example; a theoretical calculation was also carried out using the DFT method. The geometric optimizations and frequency calculations in vacuo were carried out at the level of B3LYP/3−21G, and then the single-point energies were further calculated in aqueous solution using solvation model COSMO and with a higher basis set of LanL2DZ(f)+6−311+G(2d, 2p) (LanL2DZ(f) for Ru, and 6−311+G(2d, 2p) basis set was used for the other atoms). Transition states were further confirmed by intrinsic reaction coordinate (IRC)[75,76] calculations. All calculations were performed using Gaussian 03 program packages.[77]

3. Results and Discussion

In order to easily read the paper, simple acronyms are used throughout instead of the chemical formulas, and both are shown in Appendix.

3.1. Structural Characteristics. Because of the large size of the title complexes and the corresponding computational load, we considered only the binding of the guanine molecule (the most tightly bound nucleobase) and adenine molecule (in order to compare with guanine) to the completed hydrolyzed species which are expected to be more active in vivo, that is, α-$[Ru(azpy)_2(H_2O)_2]$ (**1**-$(H_2O)_2$), *β*-$[Ru(azpy)_2(H_2O)_2]$ (**2**-$(H_2O)_2$), α-$[Ru(azpy)(bpy)(H_2O)_2]$ (**3**-$(H_2O)_2$), and *cis*-$[Ru(bpy)_2(H_2O)_2]$ (**4**-$(H_2O)_2$). The previous works have indicated that guanine N7 is the most preferred site for binding to antitumor Ru(II) complexes,[46,48] so only the N7 site of guanine and adenine was considered (hereafter called G7 and A7, respectively) in this work. Moreover, the NMR data of α-$[Ru(azpy)_2$(9-MeAde)$](PF_6)_2$ and X-ray structure of α-$[Ru(azpy)_2$(3-MeAdeH)$](PF_6)$ have shown that the coordination of adenine bases to the α-$[Ru(azpy)_2]$ moiety results in a didentate coordination via the N6 and N7 atoms.[35,36] Hence, in our calculations, the binding of imine form of 9-methyladenine (9-MeAde) to the moiety in the didentate fashion via its N6 and N7 atoms was also considered and studied.

Since so far no X-ray structure is available for Ru(II)-DNA model base adducts studied in this work, we compared the calculational structural parameters of analog *cis*-$[Ru(bpy)_2(9eguaN7)Cl]^{2+}$ with its experimental data,[37] in order to validate our calculational method. From the comparison shown in Table S2, we can find that all of the computed selective bond lengths are slightly longer than the corresponding experimental ones (1.4−4.0%), and the mean error of the computed bond angles from the experimental data is ∼1.1%. The computational differences from the experimental data can be thought as systematic errors caused by the computational method/basis set and environment factors. Therefore, the results of the full geometric optimization computations by the DFT method at B3LYP/(LanL2DZ + 6−31G(d)) level should be reliable, and on the basis of the computed geometries of the complexes, we can carry out the study on the structural analysis as well as the further study on thermodynamic properties for the binding of the Ru(II) hydrolyzed species to DNA model bases at higher basis set level.

The optimized structures of Ru(II)-DNA model base adducts are all shown in Figure 3, and the main geometrical parameters calculated for these complexes are listed in Tables S3, S4. All these complexes have essentially octahedral coordination around the Ru atom, with two 2-phenylazopyridine (azpy) or polypyridyl (bpy) ligands, one water and one base B ligands where B is a guanine or adenine (or one 9-methyladenine with didentate coordination). The hybrid species of complexes **2** and **3** can bind to base B in two different sites and results in two isomeric complexes, for example, *β*- and *β*′-$[Ru(azpy)_2(G7)(H_2O)]^{2+}$ (*β* indicates the isomer with the guanine trans to the N(azo) atom, *β*′ indicates the isomer with the guanine trans to the N(py) atom, hereafter named **2**-G7 and **2**′-G7). Hence, the isomeric complexes were also considered and calculated at the same theoretical level.

From Figure 3, we can see that, except for α′-$[Ru(azpy)(bpy)(A7)H_2O]^{2+}$ (α′ indicates the isomer with the adenine trans to the N(bpy) atom, **3**′-A7), in all of the structures of Ru-G7 and Ru-A7 adducts, the water ligands act as hydrogen-bond donors, whereas the oxo and amino groups at the C6 position of the guanine and adenine rings are hydrogen-bond acceptors. As for **3**′-A7, the amino group at the C6 position of the adenine acts as a hydrogen-bond donor and the water ligand is a hydrogen-bond acceptor. The bond length of hydrogen bond in **3**′-A7 adduct is larger (1.955 Å) when compared with that in its isomeric complex α-$[Ru(azpy)(bpy)(A7)H_2O]^{2+}$ (α indicates the isomer with the adenine trans to the N(azo) atom, **3**-A7; 1.702 Å). It implies that the amino group at the C6 position of the adenine is not a much better hydrogen-bond donor for these complexes. The Ru−N(bpy) and Ru−N(azo) bond lengths are similar for all DNA adducts. Ru−N7, Ru−O(wat.) bond lengths and hydrogen bond lengths are obviously shorter in the Ru-G7 adducts than those in the Ru-A7 adducts. This may be responsible for the stronger bond energies calculated for the Ru-G7 adducts. Since the formation of hydrogen bond, the involved O(wat.)−H1 bond (H1 is the H atom of hydrogen bond) is lengthened by 0.04−0.13 Å compared with the remaining O(wat.)−H2 bond if the hydrogen bond in **3**′-A7 is excluded. These hydrogen bonds are very similar to those observed for the corresponding guanine and adenine adducts of cisplatin, but slightly longer. For instance, the DFT calculations at the level of B3LYP/(cc-pVTZ(-f) + 6−31G**) have shown C═O···H(wat.) distances of 1.368 and 1.580 Å, respectively, for the guanine and adenine adducts of cisplatin, that is, *cis*-$[Pt(NH_3)_2(G7)H_2O]^{2+}$ and *cis*-$[Pt(NH_3)_2(A7)H_2O]^{2+}$.[73]

It has been reported that the hydrogen bonds play a very important role both in the kinetics of the binding process of Pt moiety to DNA model bases and in the stabilization of the adduct structures.[73,78–81] A similar case showing the hydrogen-bonding importance was found for the ruthenium systems.[38,48,82] Below, we will see that these H-bond characteristics closely correlate to the Ru−B bond dissociation energy of Ru(II)-DNA adducts.

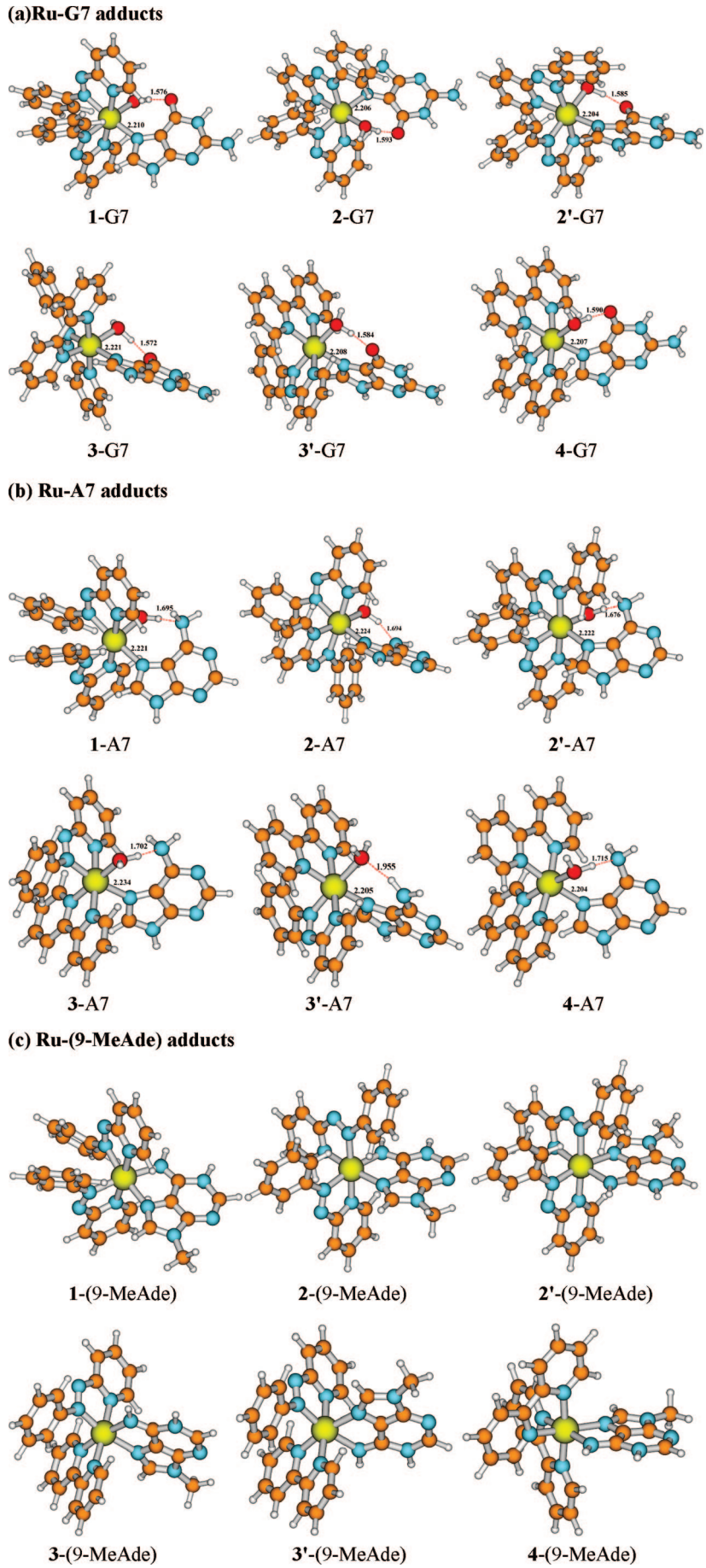

Figure 3. Optimized structures for all of the Ru(II)-DNA model base adducts studied in this work. (a) Ru-G7 adducts. (b) Ru-A7 adducts. (c) Ru-(9-MeAde) adducts.

TABLE 1: Bond Dissociation Enthalpies and Free Energies (kJ mol^{-1}) in the Gas Phase and Aqueous Solution for the Ru(II)-B Bonds in the Ru(II)-DNA Model Bases Adducts

complex	ΔH^{298} (gas)	ΔH^{298} (aq)	ΔG^{298} (gas)	ΔG^{298} (aq)	$\Delta\Delta G_{solv}$
		Ru-G7 adducts			
1-G7	255.75	94.45	194.77	33.47	−161.29
2-G7	246.67	93.04	190.10	36.47	−153.64
2′-G7	245.89	91.20	186.43	31.74	−154.68
3-G7	234.61	84.15	174.88	24.42	−150.46
3′-G7	241.65	89.40	181.91	29.65	−152.26
4-G7	237.63	85.37	178.38	26.13	−152.26
		Ru-A7 adducts			
1-A7	145.51	64.84	82.07	1.40	−80.67
2-A7	144.99	62.69	83.25	0.95	−82.30
2′-A7	151.27	59.01	87.98	−4.28	−92.26
3-A7	128.47	58.97	66.23	−3.27	−69.50
3′-A7	115.00	72.66	54.85	12.51	−42.34
4-A7	138.87	64.65	75.30	1.08	−74.22
		Ru-(9-MeAde) adducts			
1-(9-MeAde)	347.93	201.20	277.96	131.23	−146.73
2-(9-MeAde)	331.32	177.18	262.39	108.25	−154.14
2′-(9-MeAde)	329.90	174.47	268.27	112.84	−155.44
3-(9-MeAde)	333.51	181.97	270.89	119.35	−151.54
3′-(9-MeAde)	334.54	182.20	277.57	125.23	−152.34
4-(9-MeAde)	325.07	169.51	263.97	108.40	−155.56

SCHEME 1: Thermodynamical Cycle Used for Calculations of Ru−B Bond Dissociation Free Energies Taking into Account the Solvation Effect

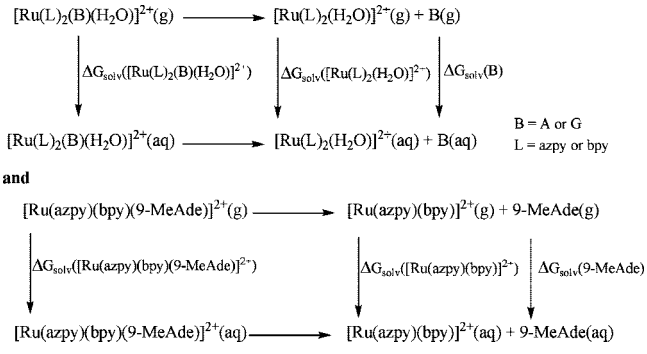

3.2. Bond Dissociation Energies. The calculated thermodynamical enthalpies, free energies and the solvation energies of Ru(II) hybrid species, Ru(II) fragments and B, as well as the corresponding values for Ru−B adducts in gas-phase and aqueous solution, are given in Tables S5 and S6. Moreover, the calculated gas-phase and solution Ru−B bond dissociation enthalpies and free energies together with the solvation energies adopting COSMO model are all listed in Table 1, the thermodynamic cycle shown in Scheme 1was adopted for calculating these data.

Since N6, N7-bidentate coordination of 9-MeAde with the Ru(II) fragments, the Ru−B bond dissociation enthalpies and free energies of Ru-(9-MeAde) adducts include the contributions of two bonds. That is the reason why the bond dissociation free energies of Ru-(9-MeAde) adducts are the largest both in the gas phase and in the aqueous solution, which are in the range of 262.39−277.96 kJ·mol^{-1} and 108.25−131.23 kJ·mol^{-1} in gas phase and in solution, respectively. In comparison with Ru-A7 adducts, the bond dissociation free energies of Ru-G7 adducts both in the gas phase and in solution are much larger; that is, those of Ru-G7 are 174.88−194.77 kJ·mol^{-1} and 24.42−36.47 kJ·mol^{-1}, whereas those of Ru-A7 are 54.85−87.98 kJ·mol^{-1} and −4.28−12.51 kJ·mol^{-1} from the gas phase to solution. The bond dissociation enthalpies and free energies reported in Table 1 indicate that these values reduce strongly from the gas phase to solution, mainly because of the high solvation energies of the charged metal fragments. The decrease is larger for the Ru-G7 adducts because of their higher solvation energies. Meanwhile, the fact that the bond dissociation free energies of Ru-A7 adducts in solution are much lower, or even become negative values, suggests that binding of hydrolyzed Ru(II) species to adenine at N7 site is a quite unfavorable process. It is also in agreement with the experimental observation that the coordination of adenine bases to the α-[Ru(azpy)$_2$] moiety results in didentate coordination via the N6 and N7 atoms.[35,36]

The Ru−B bond dissociation enthalpies and free energies of Ru(II)-G7 and Ru(II)-A7 adducts are comparable to the corresponding values calculated for the binding of these two base molecules to [Ru(NH$_3$)$_5$B]$^{2+}$ in recent computational studies.[46] For instance, at the VWN/STO(COSMO) level of theory, for [Ru(NH$_3$)$_5$(G7)]$^{2+}$, the bond dissociation free energy is 256 kJ·mol^{-1} in gas phase and is 45 kJ·mol^{-1} in solution, while for [Ru(NH$_3$)$_5$(A7)]$^{2+}$, the corresponding values are 122 kJ·mol^{-1} and −7.7 kJ·mol^{-1} respectively in gas phase and solution.[46]

More in detail, for Ru-G7 adducts, the calculated binding order is **1**-G7 > **2**-G7 > **2′**-G7 > **3′**-G7 > **4**-G7 > **3**-G7 in gas phase, while it is **2**-G7 > **1**-G7 > **2′**-G7 > **3′**-G7 > **4**-G7 > **3**-G7 in solution, showing a slight dropping behind of **1**-G7 in the binding order from gas phase to solution because of its highest solvation free energy. For Ru-(9-MeAde) adducts, the calculated binding data show the same sequence both in gas phase and in solution with **1**-(9-MeAde) > **3′**-(9-MeAde) > **3**-(9-MeAde) > **2′**-(9-MeAde) > **4**-(9-MeAde) > **2**-(9-MeAde). For Ru-A7 adducts, the calculated binding sequence is **2′**-A7 > **2**-A7 > **1**-A7> **4**-A7 > **3**-A7 > **3′**-A7 in gas phase, while this sequence almost inverts in solution. In particular, the lowest solvation free energy of **3′**-A7 makes it have the largest binding energy, and the highest solvation free energy of **2′**-A7 makes it have the smallest binding energy. In addition, compared with its isomer **3**-A7, **3′**-A7 shows the lower solvation free energy, such a fact is very likely to closely relate to the occurrence of unusual hydrogen bond in its structure (see Figure 3).

As mentioned above, from Table 1, we can find that, for all Ru(II)-DNA adducts, the bond dissociation enthalpies and free energies both in gas phase and in solution for Ru-G7 adducts are much larger than those for Ru-A7 adducts. This may be correlative to their different structural characteristics. First, the Ru−N7 bond lengths in Ru-G7 adducts are all corresponding shorter than those in Ru-A7 adducts (see Table S3). Second, all of the bond lengths of hydrogen bonds in Ru-G7 adducts are all much shorter than those in Ru-A7 adducts. Such results will make the geometric structures of Ru-G7 adducts more compact, and thus make their structures more stable. The previous calculational results have shown that guanine is superior to adenine for coordination to the diaqua adduct [Pt(NH$_3$)$_2$(H$_2$O)$_2$]$^{2+}$ both in the kinetics and in the thermodynamics.[73] Meanwhile, the theoretical studies for the binding of [Ru(NH$_3$)$_5$]$^{2+}$ moiety to DNA bases and peptides have also indicated that the guanine N7 is the preferred site for Ru(II) ammine complexes,[46] and a similar case was also found in the interaction of organometallic ruthenium(II) diamine anticancer compounds with nucleobases.[48] Our calculational results are in agreement with above theoretical studies.

In addition to the calculated bond dissociation enthalpies and free energies in gas phase and solution for the Ru-G7 and Ru-A7 adducts, in order to further explain that guanine is superior

SCHEME 2: Thermodynamical Cycle Used for Calculations of the Reaction Free Energies for the Aquo Ligand(S) Substituted by the Base B in Ru(II) Hydrolysis Species, Including the Solvation Effects

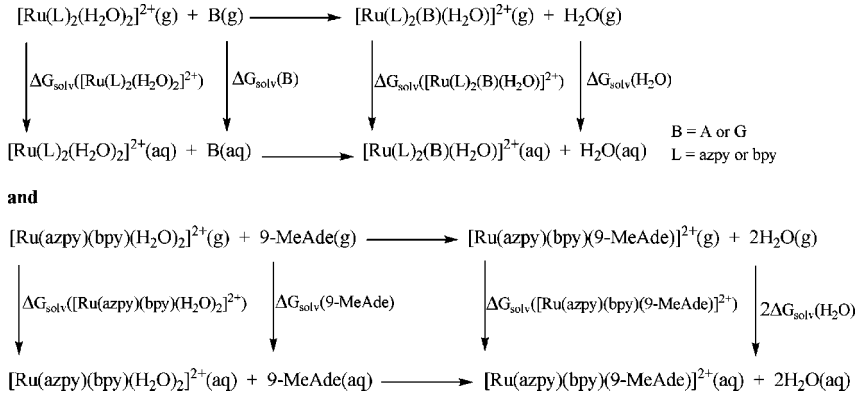

to adenine for coordination with Ru(II) hydrolyzed species, here, a kinetic study is also considered and carried out. Taking the reactions of **1**-$(H_2O)_2$ with G7 and A7 as example, the kinetic calculations were carried out using the DFT method. The fully optimized structures for the species for the two reactions are shown in Figure S1. Moreover, the calculated relative total energies, enthalpies, and free energies of the stationary points in aqueous solution, along with their solvation energies are given in Table S7, and the enthalpy and free energy profiles for the two reactions are also displayed in Figure S2. From Table S7 and Figure S2, we can see clearly that the reaction enthalpy and free energy for the reaction of **1**-$(H_2O)_2$ with A7 leading to Ru-A7 adduct are respectively larger than those for the reaction of **1**-$(H_2O)_2$ with G7, that is, 100.4 versus 91.6 kJ mol^{-1} for $\Delta H°$ in solution, and 99.2 versus 95.8 kJ mol^{-1} for $\Delta G°$ in solution. So such a conclusion that guanine N7 is superior to adenine for coordination to the diaqua Ru(II) complexes is confirmed by theoretical calculations in both thermodynamics and kinetics.

From Table 1, it should be noticed that the bond dissociation free energies of the **2**-B isomers in solution are larger than those of the **2′**-B isomers (expect for Ru-(9-MeAde) adduct), whereas those of the **3′**-B isomers in solution show stronger binding ability to DNA model bases than the **3**-B isomers. Such difference may be correlative to their isomerizations and different cytotoxicities, and it will be discussed in detail below.

3.3. Reaction Free Energies. As mentioned above, in solution, the parent Ru(II)-Cl complexes are expected to lose their chloride ligands and transform into the corresponding aquated species which then more easily undergo substitution by the DNA model bases. Moreover, the experimental and theoretical studies have proven that the completed hydrolyzed species are more active and interact easier with DNA bases.[16,19,22,42,83] Hence, it is significant to evaluate the reaction enthalpies and free energies for the water-substituted reaction by the bases A7, G7, and 9-MeAde.

The solvation effect has also been included through the COSMO model according to the reaction Scheme 2. The calculated reaction enthalpies and free energies in the gas phase and in solution are listed in Table 2. Table 2 shows that the reaction free energies for substitution of the water molecule by both bases G7 and 9-MeAde in all diaqua complexes are negative; it is consistent with the observed experimentally easy substitution of water by these bases. For the substitutive reaction of the water molecule by the base A7, the reaction free energies are positive, with the exception of the formation of **3′**-A7 and **4**-A7. It further proves that the binding of hydrolyzed Ru(II) species to adenine at the N7 site should not be a favorite process.

TABLE 2: Reaction Enthalpies and Free Energies (kJ mol^{-1}) in the Gas Phase and Aqueous Solution for the Water-Substituted Reaction by the Bases A, G, and 9-MeAde

complex	ΔH^{298} (gas)	ΔH^{298} (aq)	ΔG^{298} (gas)	ΔG^{298} (aq)	$\Delta\Delta G_{solv}$
			Ru-G7 adducts		
1-G7	−175.85	−42.13	−161.36	−27.64	133.72
2-G7	−165.37	−38.76	−150.22	−23.61	126.61
2′-G7	−164.58	−36.93	−146.54	−18.89	127.65
3-G7	−164.81	−36.86	−146.70	−18.75	127.95
3′-G7	−171.85	−42.10	−153.73	−23.99	129.75
4-G7	−160.86	−41.49	−145.06	−25.69	119.37
			Ru-A7 adducts		
1-A7	−65.61	−12.52	−48.66	4.43	53.09
2-A7	−63.68	−8.41	−43.36	11.91	55.27
2′-A7	−69.96	−4.73	−48.09	17.14	65.23
3-A7	−58.66	−11.68	−38.05	8.93	46.99
3′-A7	−45.20	−25.37	−26.67	−6.84	19.83
4-A7	−62.10	−20.76	−41.98	−0.64	41.34
			Ru-9-MeAde adducts		
1-(9-MeAde)	−182.02	−29.15	−201.56	−107.63	93.93
2-(9-MeAde)	−171.65	−26.52	−189.32	−92.92	96.40
2′-(9-MeAde)	−170.24	−31.30	−195.20	−110.06	85.14
3-(9-MeAde)	−175.19	−27.98	−196.98	−99.57	97.40
3′-(9-MeAde)	−176.21	−33.85	−203.65	−105.46	98.20
4-(9-MeAde)	−166.62	−73.78	−191.08	−98.24	92.84

The calculated reaction free energies reported in Table 2 indicate that, not only in the gas phase but also in aqueous solution, the reaction free energies for the formation of Ru-(9-MeAde) adducts are the largest (in negative), suggesting the easy substitution of water molecules by 9-MeAde and that the adducts are more stable due to its N6, N7-didentate coordination. In addition, for **1**-G7 and **1**-(9-MeAde) adducts, the reaction free energies are larger (in negative), it is also in accordance with their higher bond dissociation energies.

3.4. Inquiry of Structure−activity Relationship (SAR). The IC_{50} values of the four structurally related Ru(II) complexes **1**−**4** were determined in a series of human tumor cell lines by Hotze et al. and are given in Table S8.[9] From Table S8, we can see clearly that the trend in the antitumor activities (A) of the four structurally related complexes is A(**1**) > A(**2**) > A(**3**) > A(**4**). Hence, it is interesting to compare the striking different cytotoxicities of these four complexes, that is, the highly cytotoxic **1**, moderately cytotoxic **2**, lowly cytotoxic **3**, and inactive **4**, and then to explore the structure−activity relationship (SAR) for this kind of complex.

To explain the difference in cytotoxicity of this kind of complex, above results on DNA model base binding studies

TABLE 3: Comparison between the Gas-Phase ZPE-Corrected Energies (a.u.) and the Aqueous-Phase Single-Point Energies (a.u.) of the Considered Isomer Complexes for Their G7, 9-MeAde Adducts (1 a.u. = 27.21 eV)

complex	$E_{tot/ZPE}$(g)	E_{tot}(aq)
2-G7	−1890.1887	−1890.3636
2′-G7	−1890.1885	−1890.3629
3-G7	−1796.7719	−1976.9507
3′-G7	−1796.7748	−1976.9529
2-(9-MeAde)	−1777.7530	−1777.9236
2′-(9-MeAde)	−1777.7534	−1777.9235
3-(9-MeAde)	−1684.3388	−1684.5134
3′-(9-MeAde)	−1684.3391	−1684.5135

can be used, as it is generally thought that DNA might be the target of antitumor−active ruthenium complexes. Here, we can especially discuss the structure−activity relationship of this series of complexes.

First, thermodynamically, the Ru−B bond dissociation free energies of **1**-G7 and **1**-(9-MeAde) are almost the largest, and their reaction free energies are larger in negative, suggesting that the DNA adducts from the coordination of the hydrolyzed species of **1** are more stable thermodynamically. The largest/larger bond dissociation free energies and reaction free energies are consistent with the highest cytotoxicity of complex **1.** Meanwhile, the bond dissociation free energies of **4**-G7 and **4**-(9-MeAde) are nearly the smallest, implying that they are not stable thermodynamically; it is also in accordance with the lowest cytotoxicity (even inactivity) of complex **4**. Hence, the thermodynamical characteristics of their DNA adducts may relate closely to their distinct cytotoxicities.

Second, from Tables 1 and 2, we can find that, for the isomeric complexes **3**-B and **3′**-B, the bond dissociation free energies and reaction free energies of **3′**-B isomer (B trans to the N(bpy) atom) are all larger than those of **3**-B (B trans to the N(azo) atom) and that the ZPE-corrected total energy in gas phase ($E_{tot/ZEP}$(g)) and the total energy in aqueous solution (E_{tot}(aq)) of **3′**-B isomer are also respectively lower than those of isomer **3**-B (see Table 3), suggesting that the **3′**-B isomer is more stable thermodynamically. It further supports the experimental results of isomerization of **3-**(9-EtGua) into **3′-**(9-EtGua).[9] Hence, the low cytotoxicity of parent complex **3** can be explained by the fact that the stable *trans*-N(bpy) adduct is not advantageous to improving the activity.

In the case of the isomeric complexes **2**-G7 and **2′**-G7, the **2**-G7 isomer shows the larger bond dissociation free energies and reaction free energies, and the lower ZPE-corrected total energy in gas phase ($E_{tot/ZEP}$(g)) and total energy in aqueous solution (E_{tot}(aq)) than **2′**-G7 isomer, suggesting that the **2**-G7 isomer (G7 trans to the N(azo) atom) is more stable thermodynamically. So we can predict that **2′**-G7 might be converted into **2**-G7 isomer theoretically. This is also consistent with the experimental result that the isomerization of **2**-G7 into **2′**-G7 isomer takes place at a slow rate, even after two months in acetone-d_6 at room temperature.[39] With a combination of the moderate cytotoxicity of complex **2** and the above analysis, we can also conclude that the stable *trans*-N(azo) G7 adduct is favorable to the cytotoxicity of this kind of complex.

In addition, in DNA adducts of **1**-B and **4**-B, since both two coordination sites are equivalent, the coordination with B exists only with one site, that is, *trans*-N(azo) and *trans*-N(bpy), respectively for **1** and **4** DNA adducts. Considering the high cytotoxicity of **1** and inactivity of **4**, such a hypothesis, of the stable *trans*-N(azo) adduct as a prerequisite for a biologically high cytotoxicity, should be reasonable and acceptable.[9]

TABLE 4: Some Frontier Molecular Orbital Energies (ε_i/a.u) and Related Energy Differences ($\Delta\varepsilon$) of Antitumor Ru(II) Complexes as well as Their Completed Hydrolyzed Species

complex	H-1	HOMO[a]	LUMO[b]	L + 1	$\Delta\varepsilon_{L\text{-}H}$[c]
1	−0.2061	−0.1925	−0.1114	−0.1007	0.0811
2	−0.2026	−0.1929	−0.1103	−0.1024	0.0826
3	−0.1925	−0.1829	−0.095	−0.0815	0.0879
4	−0.1778	−0.1642	−0.0739	−0.0715	0.0903
1-$(H_2O)_2$	−0.4512	−0.4462	−0.3332	−0.3277	0.1130
2-$(H_2O)_2$	−0.4521	−0.4473	−0.3328	−0.3278	0.1145
3-$(H_2O)_2$	−0.4464	−0.4434	−0.3258	−0.2939	0.1176
4-$(H_2O)_2$	−0.4361	−0.4323	−0.2931	−0.2906	0.1392

[a] HOMO (or H): the highest occupied molecular orbital; H-1: the next HOMO. [b] LUMO (or L): the lowest unoccupied molecular orbital; L+1: the next LUMO. [c] $\Delta\varepsilon_{L\text{-}H}$: the energy difference between LUMO and HOMO.

Third, although the kinetics studies on the monofunctional binding of the completed hydrolyzed species of this series of antitumor Ru(II) complexes to purine bases were not entirely carried out in this limited work, and thus the systematical comparisons based on the kinetics were not performed yet, the comparisons among the energy differences $\Delta\varepsilon_{L\text{-}H}$ of compound molecules can be carried out as a qualitative consideration. It can be accepted that $\Delta\varepsilon_{L\text{-}H}$ is generally an important factor characterizing the reaction activity of the molecule on the kinetics;[84] that is, in general, the smaller the energy difference $\Delta\varepsilon_{L\text{-}H}$, the greater the reaction activity of the molecule is. So the energy difference $\Delta\varepsilon_{L\text{-}H}$ of the parent chloro complexes **1**−**4** as well as their hydrolyzed species were calculated in our work and reported in Table 4. From Table 4, we can see that, for both the parent chloro complexes and their hydrolyzed species, the trend in the HOMO−LUMO energy gap ($\Delta\varepsilon_{L\text{-}H}$) is $\Delta\varepsilon_{L\text{-}H}$ (**1**) < $\Delta\varepsilon_{L\text{-}H}$ (**2**) < $\Delta\varepsilon_{L\text{-}H}$ (**3**) < $\Delta\varepsilon_{L\text{-}H}$ (**4**), which is also in agreement with that in the anticancer-activity (A), that is, A(**1**) > A(**2**) > A(**3**) > A(**4**). Hence, the striking difference in activity among the four complexes is further explained theoretically.

At present, the reasons behind the differences in cytotoxicity of this series of structurally related complexes **1**-**4** are still far from being understood; many factors might affect the biological activity, for example, the coordination to biological target (DNA, etc.), differences of uptake and transport into cells among the drug molecules,[6] and other physicochemical properties.[85] However, in this paper, the geometric structures and thermodynamical characteristics of the DNA model base adducts are studied from quantum-chemical insight, and the possible SAR is obtained. In line with the results and findings obtained in this study, further work is now in progress aiming to explore the kinetics processes for the binding of the hydrolyzed products of Ru(II) antitumor complexes to DNA bases.

4. Conclusions

In this work, the thermodynamics of the binding of a series of structurally related Ru(II) antitumor complexes to DNA purine bases has been studied using the DFT method. The theoretical results show the following: (1) The hydrogen bond characteristic plays a very important role both in the stabilization of the DNA adducts and in the Ru−B bond dissociation free energies.

(2) For all Ru(II)-DNA model base adducts studied in this work, the bond dissociation enthalpies and free energies both in the gas phase and in solution for Ru-G7 adducts are much larger than those observed for Ru-A7 adducts, suggesting that

the guanine N7 is a preferred site for this series of complexes. In addition, the reaction free energies for the formation of Ru-(9-MeAde) adducts are the largest, indicating that the water ligand in hybrid species is more easily substituted by 9-MeAde and that the adducts being more stable can be attributed to the N6, N7-didentate coordination.

(3) The Ru−B bond dissociation free energies of **1**-B, in particular, **1**-G7 and **1**-(9-MeAde) are almost the largest and their reaction free energies are larger in negative. On the contrary, the bond dissociation free energies of **4**-G7 and **4**-(9-MeAde) are nearly the smallest. Such results are consistent with the highest and lowest cytotoxicities of their parent complexes **1** and **4**, respectively.

(4) Via comparing the total energies and the bond dissociation free energies as well as reaction free energies of isomeric complexes **3**-B and **3′**-B, **2**-G7 and **2′**-G7, the calculational results further support the isomerization of **3**-(9-EtGua) into **3′**-(9-EtGua) observed experimentally, and thus suggest that the stable *trans*-N(azo) adduct is favorable to the cytotoxicity of this kind of complex.

(5) On the basis of structural and thermodynamical characteristics, the possible SAR is obtained, and the striking difference in cytotoxicity of this series of structurally related antitumor complexes is explained theoretically.

Appendix

Abbreviations

Acronym, Chemical Formula

1,	α-[Ru(azpy)$_2$Cl$_2$]
2,	*β*-[Ru(azpy)$_2$Cl$_2$]
3,	α-[Ru(azpy)(bpy)Cl$_2$]
4,	*cis*-[Ru(bpy)$_2$Cl$_2$]
1-(H$_2$O)$_2$,	α-[Ru(azpy)$_2$(H$_2$O)$_2$]$^{2+}$
2-(H$_2$O)$_2$,	*β*-[Ru(azpy)$_2$(H$_2$O)$_2$]$^{2+}$
3-(H$_2$O)$_2$,	α-[Ru(azpy)(bpy)(H$_2$O)$_2$]$^{2+}$
4-(H$_2$O)$_2$,	*cis*-[Ru(bpy)$_2$(H$_2$O)$_2$]$^{2+}$
1-G7,	α-[Ru(azpy)$_2$(G7)H$_2$O]$^{2+}$
2-G7,	*β*-[Ru(azpy)$_2$(G7)H$_2$O]$^{2+}$
2′-G7,	*β′*-[Ru(azpy)$_2$(G7)H$_2$O]$^{2+}$
3-G7,	α-[Ru(azpy)(bpy)(G7)H$_2$O]$^{2+}$
3′-G7,	α′-[Ru(azpy)(bpy)(G7)H$_2$O]$^{2+}$
4-G7,	*cis*-[Ru(bpy)$_2$(G7)H$_2$O]$^{2+}$
1-A7,	α-[Ru(azpy)$_2$(A7)H$_2$O]$^{2+}$
2-A7,	*β*-[Ru(azpy)$_2$(A7)H$_2$O]$^{2+}$
2′-A7,	*β′*-[Ru(azpy)$_2$(A7)H$_2$O]$^{2+}$
3-A7,	α-[Ru(azpy)(bpy)(A7)H$_2$O]$^{2+}$
3′-A7,	α′-[Ru(azpy)(bpy)(A7)H$_2$O]$^{2+}$
4-A7,	*cis*-[Ru(bpy)$_2$(A7)H$_2$O]$^{2+}$
1-(9-MeAde),	α-[Ru(azpy)$_2$(9-MeAde)]$^{2+}$
2-(9-MeAde),	*β*-[Ru(azpy)$_2$(9-MeAde)]$^{2+}$
2′-(9-MeAde),	*β′*-[Ru(azpy)$_2$(9-MeAde)]$^{2+}$
3-(9-MeAde),	α-[Ru(azpy)(bpy)(9-MeAde)]$^{2+}$
3′-(9-MeAde),	α′-[Ru(azpy)(bpy)(9-MeAde)]$^{2+}$
4-(9-MeAde),	*cis*-[Ru(bpy)$_2$(9-MeAde)]$^{2+}$
3-(9-EtGua),	α-[Ru(azpy)(bpy)(9-EtGua)H$_2$O]$^{2+}$
3′-(9-EtGua),	α′-[Ru(azpy)(bpy)(9-EtGua)H$_2$O]$^{2+}$

Acknowledgment. The financial supports of the National Natural Science Foundation of China and the Natural Science Foundation of Guangdong Province of China are gratefully acknowledged. Meanwhile, we thank the Information & Network Center, Sun Yat-Sen University for offering the High Performance Computing Clusters (HPCC).

Supporting Information Available: Test calculation of solvation free energies in aqueous solution for adenine and guanine (Table S1); comparison between calculated and experimental geometrical parameters for *cis*-[Ru(bpy)$_2$(9eguaN^7)Cl]$^+$ (Table S2); main geometrical parameters calculated for the Ru-G7, Ru-A7 and Ru-(9-MeAde) adducts (Tables S3, S4); the calculated thermodynamical energies of Ru(II) hybrid species, Ru(II) fragments and B as well as the corresponding values for Ru−B adducts (Tables S5, S6); calculated relative total energies, enthalpies, free energies, solvation free energies for the species of the two reactions of **1**-(H$_2$O)$_2$ + G7(A7) (Table S7); the IC_{50} values of title complexes against human tumor-cell lines (Table S8); optimized structures for the stationary points and enthalpy and free energy profile for the reactions of **1**-(H$_2$O)$_2$ +G7(A7) (Figures S1, S2). This information is available free of charge via the Internet at http://pubs.acs.org.

References and Notes

(1) Wong, E.; Giandomenico, C. M. *Chem. Rev.* **1999**, *99*, 2451.
(2) Clarke, M. J. In *Metal Complexes in Cancer Chemotherapy;* Keppler, B. K., Ed.; VCH: Weinheim, 1993; p 129.
(3) Keppler, B. K.; Lipponer, K-G.; Stenzel, B. and Kratz, F. In *Metal Complexes in Cancer Chemotherapy*; Keppler, B. K., Ed.; VCH: Weinheim, 1993; p 187.
(4) Clarke, M. J.; Zhu, F.; Frasca, D. R. *Chem. Rev.* **1999**, *99*, 2511.
(5) Sava, G.; Bergamo, A. *Int. J. Oncol.* **2000**, *17*, 353.
(6) Hotze, A. C. G.; Caspers, S. E.; de Vos, D.; Kooijman, H.; Spek, A. L.; Flamigni, A.; Bacac, M.; Sava, G.; Haasnoot, J. G.; Reedijk, J. *J. Biol. Inorg. Chem.* **2004**, *9*, 354.
(7) Velders, A. H.; Kooijman, H.; Spek, A. L.; Haasnoot, J. G.; de Vos, D.; Reedijk, J. *Inorg. Chem.* **2000**, *39*, 2966.
(8) Nováková, O.; Kašpárková, J.; Vrána, O.; van Vliet, P. M.; Reedijk, J.; Brabec, V. *Biochemistry* **1995**, *34*, 12369.
(9) Hotze, A. C. G.; van der Geer, E. P. L.; Caspers, H. K.; Spek, A. L.; Haasnoot, J. G.; Reedijk, J. *Inorg. Chem.* **2004**, *43*, 4935.
(10) Jamieson, E. R.; Lippard, S. J. *Chem. Rev.* **1999**, *99*, 2467.
(11) Howe-Grant, M.; Lippard, S. J. *Metal Ions Biol. Syst.* **1980**, *11*, 63.
(12) Pavelka, M.; Lucas, M. F. A.; Russo, N. *Chem. Eur. J.* **2007**, *13*, 10108.
(13) Suvachittanont, S.; van Eldik, R. *Inorg. Chem.* **1994**, *33*, 895.
(14) Suvachittanont, S.; Hohmann, H.; van Eldik, R.; Reedijk, J. *Inorg. Chem.* **1993**, *32*, 4544.
(15) Hohmann, H.; Hellquist, B.; Van Eldik, R. *Inorg. Chem.* **1992**, *31*, 1090.
(16) Holler, E.; Schaller, W.; Keppler, B. K. *Arzneim.-Forsch./Drug Res.* **1991**, *41*, 1065.
(17) Clarke, M. J.; Zhu, F.; Frasca, D. R. *Chem. Rev.* **1999**, *99*, 2511.
(18) Sava, G.; Alessio, E.; Bergamo, A. and Mestroni, G. In *Topics in Biological Inorganic Chemistry*; Clarke, M. J., Sadler, P. J., Eds.; Springer: Berlin, 1999; p 143.
(19) Mestroni, G.; Alessio, E.; Sava, G.; Pacor, S.; Coluccia, M.; Bocarelli, A. *Metal Based Drugs* **1994**, *1*, 41.
(20) Sava, G.; Alessio, E.; Bergamo, A.; Mestroni, G. In *Biological Inorganic Chemistry*; Clarke, M. J., Sadler, P. J., Eds.; Springer-Verlag: Berlin, 1999; Vol. 1, p 154.
(21) Savaa, G.; Bergamoa, A.; Zorzetb, S.; Gavaa, B.; Casarsaa, C.; Cocchiettoa, M.; Furlanib, A.; Scarciab, V.; Serlic, B.; Iengoc, E.; Alessioc, E.; Mestronic, G. *Eur. J. Cancer* **2002**, *38*, 427.
(22) Messori, L.; Kratz, F.; Alessio, E. *Metal Based Drugs* **1996**, *3*, 1.
(23) Küng, A.; Pieper, T.; Wissiack, R.; Rosenberg, E.; Keppler, B. K. *J. Biol. Inorg. Chem.* **2001**, *6*, 292.
(24) Chatlas, J.; van Eldik, R.; Keppler, B. K. *Inorg. Chim. Acta* **1995**, *233*, 59.
(25) Ni Dhubhghaill, O. M.; Hagen, W. R.; Keppler, B. K.; Lipponer, K. G.; Sadler, P. J. *Dalton Trans.* **1994**, *22*, 3305.
(26) Anderson, C.; Beauchamp, A. L. *Can. J. Chem.* **1995**, *73*, 471.
(27) Clarke, M. J. *Coord. Chem. Rev.* **2002**, *232*, 69.
(28) Velders, A. H.; Hotze, A. C. G.; van Albada, G. A.; Haasnoot, J. G.; Reedijk, J. *Inorg. Chem.* **2000**, *39*, 4073.
(29) Brabec, V.; Novakova, O. *Drug Resistance Update* **2006**, *9*, 111.
(30) Kuehn, C. G.; Taube, H. *J. Am. Chem. Soc.* **1976**, *98*, 689.
(31) Fruhauf, S.; Zeller, W. J. *Cancer Res.* **1991**, *51*, 2943.
(32) Gallori, E.; Vettori, C.; Alessio, E.; Vilchez, F. G.; Vilaplana, R.; Orioli, P.; Casini, A.; Messori, L. *Arch. Biochem. Biophys.* **2000**, *376*, 156.

(33) Clarke, M. J.; Jansen, B.; Marx, K. A.; Kruger, R. *Inorg. Chim. Acta* **1986**, *124*, 13.
(34) McNamara, M. A.; Clarke, M. J. *Inorg. Chim. Acta* **1992**, *195*, 175.
(35) Hotze, A. C. G.; Broekhuisen, M. E. T.; Velders, A. H.; Kooijman, H.; Spek, A. L.; Haasnoot, J. G.; Reedijk, J. *J. Chem. Soc. Dalton Trans.* **2002**, *14*, 2809.
(36) Hotze, A. C. G.; Broekhuisen, M. E. T.; van der Schilden, K.; Haasnoot, A. H.; Reedijk, J. G. J. *Eur. J. Inorg. Chem.* **2002**, *2*, 369.
(37) van Vliet, P. M.; Haasnoot, J. G.; Reedijk, J. *Inorg. Chem.* **1994**, *33*, 1934.
(38) Hotze, A. C. G.; Velders, A. H.; Ugozzoli, F.; Biagini-Cingi, M.; Manotti-Lanfredi, A. M.; Haasnoot, J. G.; Reedijk, J. *Inorg. Chem.* **2000**, *39*, 3838.
(39) Velders, A. H. PhD thesis, Leiden University, 2000.
(40) Velders, A. H.; Gomez Quiroga, A.; Haasnoot, J. G.; Reedijk, J. *Eur. J. Inorg. Chem.* **2003**, *4*, 713.
(41) Velders, A. H.; Hotze, A. C. G.; Haasnoot, J. G.; Reedijk, J. *Inorg. Chem.* **1999**, *38*, 2762.
(42) Chen, J. C.; Chen, L. M.; Liao, S. Y.; Zheng, K. C.; Ji, L. N. *Dalton Trans.* **2007**, *32*, 3507.
(43) Chen, J. C.; Chen, L. M.; Liao, S. Y.; Zheng, K. C.; Ji, L. N. *J. Phys. Chem. B* **2007**, *111*, 7862.
(44) Chen, J. C.; Li, J.; Wu, W. J.; Zheng, K. C. *Acta Phys. -Chim. Sin.* **2006**, *22*, 391.
(45) Chen, J. C.; Li, J.; Qian, L.; Zheng, K. C. *J. Mol. Struct. (THEOCHEM)* **2005**, *728*, 93.
(46) Bešker, N.; Coletti, C.; Marrone, A.; Re, N. *J. Phys. Chem. B* **2007**, *111*, 9955.
(47) Wang, F.; Habtemariam, A.; van der Geer Erwin, P. L.; Fernandez, R.; Melchart, M.; Deeth, R. J.; Aird, R.; Guichard, S.; Fabbiani, F. P. A.; Lozano-Casal, P.; Oswald, I. D. H.; Jodrell, D., I.; Parsons, S.; Sadler, P. J. *Proc. Natl. Acad. Sci. U.S.A.* **2005**, *102*, 18269.
(48) Gossens, C.; Tavernelli, I.; Rothlisberger, U. *J. Chem. Theory Comput.* **2007**, *3*, 1212.
(49) Foresman, J. B.; Frisch, Æ. In *Exploring Chemistry with Electronic Structure Methods*, 2nd ed., Gaussian Inc.: Pittsburgh, PA, 1996.
(50) Hohenberg, P.; Kohn, W. *Phys. Rev. B* **1964**, *136*, 864.
(51) Becke, A. D. *J. Chem. Phys.* **1993**, *98*, 1372.
(52) Görling, A. *Phys. Rev. A* **1996**, *54*, 3912.
(53) Becke, A. D. *J. Chem. Phys.* **1993**, *98*, 5648.
(54) Lee, C.; Yang, W.; Parr, R. G. *Phys. Rev. B* **1988**, *37*, 785.
(55) Juris, A.; Balzani, V.; Barigelletti, F.; Campagna, S.; Belser, P.; Zelewsky, A. V. *Coord. Chem. Rev.* **1988**, *84*, 85.
(56) Hay, P. J.; Wadt, W. R. *J. Chem. Phys.* **1985**, *82*, 270.
(57) Wadt, W. R.; Hay, P. J. *J. Chem. Phys.* **1985**, *82*, 284.
(58) Wadt, W. R.; Hay, P. J. *J. Chem. Phys.* **1985**, *82*, 299.
(59) Ditchfield, R.; Hehre, W. J.; Pople, J. A. *J. Chem. Phys.* **1971**, *54*, 724.
(60) Hehre, W. J.; Ditchfield, R.; Pople, J. A. *J. Chem. Phys.* **1972**, *56*, 2257.
(61) Klamt, A.; Schüürmann, G. *J. Chem. Soc., Perkin Trans. 2* **1993**, *5*, 799.
(62) Pye, C. C.; Ziegler, T. *Theor. Chem. Acc.* **1999**, *101*, 396.
(63) Ehlers, A. W.; Böhme, M.; Dapprich, S.; Gobbi, A.; Höllwarth, A.; Jonas, V.; Köhler, K. F.; Stegmann, R.; Veldkamp, A.; Frenking, G. *Chem. Phys. Lett.* **1993**, *208*, 111.
(64) Barone, V.; Cossi, M. *J. Phys. Chem. A* **1998**, *102*, 1995.
(65) Cossi, M.; Rega, N.; Scalmani, G.; Barone, V. *J. Comput. Chem.* **2003**, *24*, 669.
(66) Andzelm, J.; Kölmel, C.; Klamt, A. *J. Chem. Phys.* **1995**, *103*, 9312.
(67) Elcock, A. H.; Richards, W. G. *J. Am. Chem. Soc.* **1993**, *115*, 7930.
(68) Bash, P. A.; Singh, U. C.; Langridge, R.; Kollman, P. A. *Science* **1987**, *236*, 564.
(69) Miller, J. L.; Kollman, P. A. *J. Phys. Chem.* **1996**, *100*, 8587.
(70) Cramer, C. J.; Truhlar, D. G. *Chem. Phys. Lett.* **1993**, *202*, 567.
(71) Orozco, M.; Luque, F. J. *Biopolymers* **1993**, *33*, 1851.
(72) Mohan, V.; Davis, M. E.; McCammon, J. A.; Pettitt, B. M. *J. Phys. Chem.* **1992**, *96*, 6428.
(73) Baik, M. H.; Friesner, R. A.; Lippard, S. J. *J. Am. Chem. Soc.* **2003**, *125*, 14082.
(74) Petrov, A. S.; Pack, G. R.; Lamm, G. *J. Phys. Chem. B* **2004**, *108*, 6072.
(75) Fukui, K. *Acc. Chem. Res.* **1981**, *14*, 363.
(76) Gonzalez, C.; Schlegel, H. B. *J. Chem. Phys.* **1989**, *90*, 2154.
(77) Frisch, M. J.; Trucks, G. W.; Schlegel, H. B.; Scuseria, G. E.; Robb, M. A.; Cheeseman, J. R.; Montgomery, J. A., Jr.; Vreven, T.; Kudin, K. N.; Burant, J. C.; Millam, J. M.; Iyengar, S. S.; Tomasi, J.; Barone, V.; Mennucci, B.; Cossi, M.; Scalmani, G.; Rega, N.; Petersson, G. A.; Nakatsuji, H.; Hada, M.; Ehara, M.; Toyota, K.; Fukuda, R.; Hasegawa, J.; Ishida, M.; Nakajima, T.; Honda, Y.; Kitao, O.; Nakai, H.; Klene, M.; Li, X.; Knox, J. E.; Hratchian, H. P.; Cross, J. B.; Bakken, V.; Adamo, C.; Jaramillo, J.; Gomperts, R.; Stratmann, R. E.; Yazyev, O.; Austin, A. J.; Cammi, R.; Pomelli, C.; Ochterski, J. W.; Ayala, P. Y.; Morokuma, K.; Voth, G. A.; Salvador, P.; Dannenberg, J. J.; Zakrzewski, V. G.; Dapprich, S.; Daniels, A. D.; Strain, M. C.; Farkas, O.; Malick, D. K.; Rabuck, A. D.; Raghavachari, K.; Foresman, J. B.; Ortiz, J. V.; Cui, Q.; Baboul, A. G.; Clifford, S.; Cioslowski, J.; Stefanov, B. B.; Liu, G.; Liashenko, A.; Piskorz, P.; Komaromi, I.; Martin, R. L.; Fox, D. J.; Keith, T.; Al-Laham, M. A.; Peng, C. Y.; Nanayakkara, A.; Challacombe, M.; Gill, P. M. W.; Johnson, B.; Chen, W.; Wong, M. W.; Gonzalez, C.; Pople, J. A. *Gaussian 03* Revision D.1; Gaussian, Inc.: Waliingford, CT, 2005.
(78) Reedijk, J. *Proc. Natl. Acad. Sci. U.S.A.* **2003**, *100*, 3611.
(79) Chval, Z.; Sip, M. *Collect. Czech. Chem. Commun.* **2003**, *68*, 1105.
(80) Reedijk, J. *Inorg. Chim. Acta* **1992**, *200*, 873.
(81) van Kralingen, C. G.; Reedijk, J. *Ciencia Biol.* **1980**, *5*, 159.
(82) Velders, A. H.; Ugozzoli, F.; Biagini-Cingi, M.; Manotti-Lanfredi, A. M.; Haasnoot, J. G.; Reedijk, J. *Eur. J. Inorg. Chem.* **1999**, *2*, 213.
(83) Kratz, F.; Hartmann, M.; Keppler, B. K.; Messori, L. *J. Biol. Chem.* **1994**, *269*, 2581.
(84) Aihara, J. I. *Theor. Chem. Acc.* **1999**, *102*, 134.
(85) Velders, A. H.; Van der Schilden, K.; Hotze, A. C. G.; Reedijk, J.; Kooijman, H.; Spek, A. L. *J. Chem. Soc., Dalton Trans.* **2004**, *3*, 448.

JP711799G